Variable Bias Type AMB Flywheel Powered Electric Vehicle without any Touchdown against Load Disturbance

Budi Rachmanto[1,a], Kenzo Nonami[1,b], Yuki Hiura[1,c], Takahiro Kagamiishi[1,d]
[1]Dept. of Mech. Eng., Chiba university, 1-33 Yayoi-cho, Inage-ku, Chiba 263-8522, Japan
[a]rac@graduate.chiba-u.jp, [b]nonami@faculty.chiba-u.jp, [c]y_hiura_0513@graduate.chiba-u.jp,
[d]t-kagami@graduate.chiba-u.jp

Abstract: This paper deals with a stabilization control of active magnetic bearings (AMBs). Conventionally, zero bias method was chosen in stabilization control for its advantage in minimizing stabilization energy. However stiffness of the method is low, and touchdown may occur when the vehicle moves at high acceleration rate. We introduce bias current in fixed or variable rate using generalized switching rule for zero/nonzero bias control with regards to current saturation. Depending on external disturbance, it acts as a zero bias controller or bias controller.

Keywords: Active Magnetic Bearing, Flywheel Energy Storage System, Simple Adaptive Control, Variable Bias

Introduction

Fossil fuels are limited energy and will dry up in the future. On the other hand, energy consumption certainly increases year by year, urging us to develop new energy resources while considering efficient utilization of the existing ones. Usage of flywheel energy storage system (FESS) to store electricity is one solution for energy utilization. Differs from lead batteries, it is environmentally clean, does not contain any harmful chemical substances, and can be used semi permanently as a pollution-free battery.

In our research group, there have been many studies for years regarding magnetic bearing flywheel for electricity storages. Magnetic bearing is contactless, and there are extremely little energy losses by friction. However, control is necessary to stabilize the levitation. Therefore we have been so far focusing on stabilization control of the flywheel.

As a replacement of conventional lead storage battery, and in order to broader the usage of magnetic bearing flywheel as electric energy storage, it is necessary to bring mobile FESS into reality[1], i.e. application towards moving apparatus such as ships, space/air crafts, and rail/road vehicles. We decided to realize this idea and began to develop a mobile type of FESS for vehicle application.

System Configuration

System Platform. Figure 1 shows the outlook of the electric vehicle (EV) and FESS. The platform is golf cart, with specifications listed in Table 1. Six units of lead batteries, 186kg in total, are placed under the front seat. The FESS is suspended by mechanical gimbal under the rear seat.

Flywheel System. As shown in Fig.2, the AMB flywheel has two pairs of electromagnets facing each other surrounding rotor in radial direction, installed in right angle both on the upper and lower side. Including the pair

Fig. 1 Overview of AMB Flywheel Powered EV

Table 1 Vehicle Specifications

Parameter	Value	Parameter	Value
total length	3560 mm	dry weight	360 kg
total width	1240 mm	passengers	5
total height	1860 mm	maximum load	50 kg

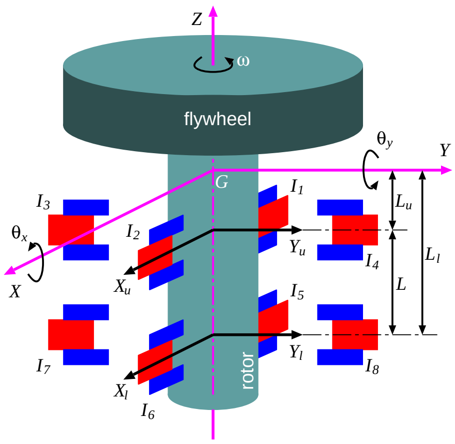

Fig. 2 Coordinates of flywheel-rotor system with homopolar AMBs

Table 2 Parameters of flywheel rotor-AMB

Parameter	Value	Unit
Moment of inertia about z axis (I_z)	1.86×10^{-1}	kgm^2
Constant of upper AMB attractive force (K_u)	3.10×10^{-6}	Nm^2/A^2
Constant of lower AMB attractive force (K_l)	4.47×10^{-6}	Nm^2/A^2
Nominal air gap (X_0, Y_0)	0.2×10^{-3}	m
Bias Current (I_0)	$0 \cdots 0.75$	A

used in axial direction, these electromagnets constitute an AMB flywheel system with 5 degrees of freedom. Sensors are installed to measure the rotor position, one per each degree of freedom. Stabilization control is performed by controlling electromagnet forces. The parameters are listed in Table 1.

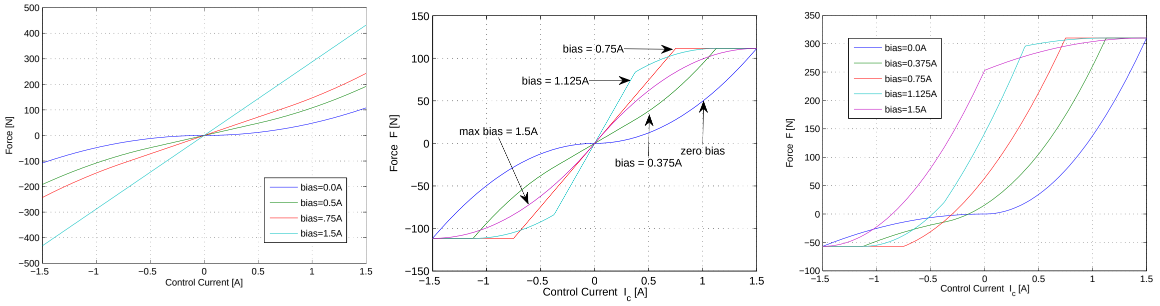

(a) non-saturated ($X_u \simeq 0$) (b) subject to current saturation ($X_u \simeq 0$) (c) saturated current mode ($X_u > 0$)

Fig. 3 Zero bias and non-zero bias characteristics

Linearity Analysis of Interacting Forces in Saturated Mode

Using basic policy of control current

$$I_{c_i} = -I_{c_{i+1}}. \qquad (i = 1,3,5,7) \tag{1}$$

$$I_i = I_0 + I_{c_i} \geq 0. \quad (i = 1,\cdots,8) \tag{2}$$

neglecting gravity, the resultant force generated by a pair of electromagnets is given by

$$F_{xu} = F_2 - F_1 = \frac{K_u(I_0+I_c)^2}{(|X_0|-X_u)^2} - \frac{K_u(I_0-I_c)^2}{(|X_0|+X_u)^2}. \tag{3}$$

Without saturation constraint, when rotor is close to the origin ($X_u \simeq 0$), the higher the bias, the better the linearity, as described in Fig.3(a). In short, for zero-bias operation, there is a "dead zone" near the origin. This is the main reason introducing bias current. As the bias raises, the slope at the origin gets steeper, leading to better dynamic response of the AMB, achieved however, at higher power losses.

With regards to the saturation current I_{max}, the force will bound as in Fig.3(b). In this condition, the control current ranges as $|I_c| \leq \frac{I_{max}}{2}$. For $I_0 > \frac{I_{max}}{2}$, despite the curve inclination around the origin goes further steeper, resulting in quicker response and higher stiffness, the linearity range shrinks back as the total current saturates faster. However, even one electromagnet got saturated, one can still hold the control by reducing bias current, as seen ultimately at $I_0 = I_{max} = 1.5$A. The slope of resultant force is maximum at the origin and goes to zero at both edges, just the contrary of zero bias case which is zero at the origin and maximum at the edges. As illustrated in Fig.3(c), non-linearity increases as the rotor moves away from the origin. Next section describes the control input considering these force/current characteristics.

Force to Current Conversion

General Switching for Saturable System. In saturable system, where the force is limited to

$$F_{max} = \frac{K_u {I_{max}}^2}{(|X_0|-X_u)^2}. \tag{4}$$

$$F_{min} = -\frac{K_u {I_{max}}^2}{(|X_0|+X_u)^2}. \tag{5}$$

a general solution for force based control input determination can be obtained by solving Eq.3:

$$I_c = \frac{\mathrm{sign}(x)\sqrt{|x|}({X_0}^2-{X_u}^2) - I_0({X_0}^2+{X_u}^2)}{2|X_0|X_u}. \qquad \left(x = \frac{F_{xu}|X_0|X_u}{K_u} + {I_0}^2\right) \tag{6}$$

especially when $X_u \simeq 0$, it becomes fully linear as

$$I_c = \frac{F_{xu} {X_0}^2}{4K_u I_0}. \tag{7}$$

then now regarding current saturation, the following switching rule is applied to the above control current:
if $I_c \geq I_0$ then

$$I_c = (|X_0| - X_u)\sqrt{\frac{F_{xu}}{K_u}} - I_0. \tag{8}$$

else if $I_c \geq I_{max} - I_0$ then

$$I_c = I_0 - (|X_0| + X_u)\sqrt{\frac{F_{max} - F_{xu}}{K_u}}. \tag{9}$$

else if $I_c \leq -I_0$ then

$$I_c = I_0 - (|X_0| + X_u)\sqrt{\frac{-F_{xu}}{K_u}}. \tag{10}$$

else if $I_c \leq I_0 - I_{max}$ then

$$I_c = (|X_0| - X_u)\sqrt{\frac{F_{xu} - F_{min}}{K_u}} - I_0. \tag{11}$$

endif

Multi-Input Multi-Output Simple Adaptive Control for Magnetic Bearings

Using conventional PD or PID control methods, when the flywheel is accelerating or decelerating, the system dynamics might change. With fixed feedback gain, the performance may deteriorate, and the influence of gyroscopic effects may become remarkable.
On this account, a speed sensor was used to detect the rotation speed of the flywheel, and based on this, gain parameters are adjusted. Improved gain scheduling techniques had been introduced in the past. Meanwhile, SAC suggested here requires no speed sensor as the gain parameters are adjusted adaptively[2] [3].
In SAC, auto-adjustment of gain parameters are originally based on PI adaptive identification rule. Here, for a quicker response, derivative rule is added. Also, as the aim is to regulate rotor position to zero, reference model is omitted. As shown in Fig.4(a), SAC here merely performs gain parameter adjustment towards output error feedback to achieve $\lim_{t\to\infty} e_y(t) = 0$. Hence, control input can be constructed as:

$$u_p(t) = K(t)z(t). \tag{12}$$

$$z(t) = e_y(t). \tag{13}$$

$$K(t) = K_P(t) + K_I(t) + K_D(t). \tag{14}$$

$$K_P(t) = -e_y(t)z(t)^T\Gamma_P. \tag{15}$$

$$\dot{K}_I(t) = -e_y(t)z(t)^T\Gamma_I - \sigma_I(t)K_I(t). \tag{16}$$

$$K_D(t) = -\frac{de_y(t)}{dt}z(t)^T\Gamma_D. \tag{17}$$

$$\sigma_I(t) = \sigma_1 \frac{e_y(t)^T e_y(t)}{1 + e_y(t)^T e_y(t)} + \sigma_2. \tag{18}$$

where $\sigma_1, \sigma_2 > 0$, $\Gamma_I, \Gamma_P, \Gamma_D$ are positive definitive symmetric gain matrices.
The control input $U = [F_{xu} \;\; F_{xl} \;\; F_{yu} \;\; F_{yl}]^T \approx u_p(t)$ is given in the form of attractive force between electromagnets, and should be converted into the form of electric current, using these switching rules. Fig.4(b) shows MIMO-SAC with bias current in AMB systems.

Bias Current Injection

Bias current can be fixed to some certain values. However, it is desired to minimize the energy for stabilization control[4]. In our system, the greatest factor causing the flywheel to touchdown is sudden speed change of the car. Bias current can be adjusted according to car acceleration rate if it can be measured using acceleration sensors or predicted beforehand.

Variable Bias Injection Using PID Mechanism. On the current system there is no acceleration sensor available. However, acceleration rate can be estimated using displacement sensors of the AMB flywheel system, by calculating the acceleration rate imposed to the flywheel rotor when the vehicle moves.

$$r(t) = \frac{\sqrt{X_u^2 + Y_u^2} + \sqrt{X_l^2 + Y_l^2}}{2}. \quad (19)$$

$$v(t) = \dot{r}(t). \quad (20)$$

$$a(t) = \dot{v}(t). \quad (21)$$

Here, bias current is chosen in such that $\lim_{t\to\infty} a(t) = 0$ using the following PID adjustment rule:

$$I_o(t) = K_{B_P} a(t) + K_{B_I} v(t) + K_{B_D} \dot{a}(t). \quad (22)$$

Adaptive Bias Injection. The variable bias above can be performed adaptively by modifying Eq.22 as:

$$I_o(t) = K_B(t) a(t). \quad (23)$$

$$K_B(t) = K_{B_P}(t) + K_{B_I}(t). \quad (24)$$

$$K_{B_P}(t) = a(t)^2 \Gamma_{B_P}. \quad (25)$$

$$\dot{K}_{B_I}(t) = a(t)^2 \Gamma_{B_I} + \sigma_{B_I}(t) K_{B_I}(t). \quad (26)$$

$$\sigma_{B_I}(t) = \sigma_{B_1} \frac{a(t)^2}{1 + a(t)^2} + \sigma_{B_2}. \quad (27)$$

provided that $\sigma_{B_1}, \sigma_{B_2}, \Gamma_{B_P}, \Gamma_{B_I} > 0$.

Experiments

Running and responsibility tests have been performed to examine the proposed methods. The experiments were done on zero bias mode, then with fixed bias and variable/adaptive bias. Figure 5 shows the time history of flywheel rotor displacements when the car is speeding up or slowing down. On zero bias mode, the flywheel is swaying greatly, increasing the probability of touchdown. With constant bias or with variable/adaptive bias, the vibration of the flywheel becomes smaller.
Figure 6 shows the time series graph of the other experiments under the gimbal restoring force. The force is raised by removing the constant moment load. The variable bias injection is clearly benefitical from Fig.6. Furthermore, variable bias pulled in input voltage as small as zero bias method.

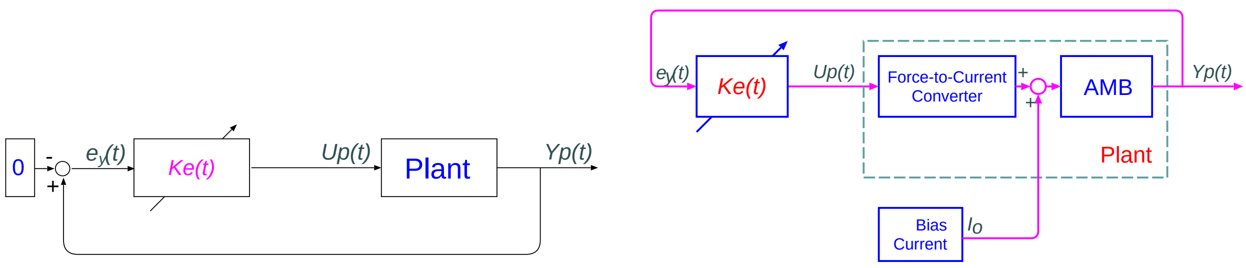

(a) with Zero Bias (b) with Bias Current

Fig. 4 MIMO-SAC for AMB

Conclusion

From these results, proposal method is improved in control and held down in power. Consequently, it can be seen that in AMB systems on moving bodies such as electric vehicles, our proposal of MIMO-SAC with variable bias is applicable.

References

[1] Budi Rachmanto, et. al., ”Energy Storage AMB Flywheel Powered Electric Vehicle”, *Dynamics and Design Conference 2009, CD-ROM Proc.*, 451, The Japan Soc. of Mech. Eng., Aug. 2009 (in Japanese).

[2] Budi Rachmanto and Kenzo Nonami, ”Zero Bias Simple Adaptive Control on Low-Loss Homopolar AMB Flywheel, A MIMO Control with PID Adaptive Identification”, *JSME Technical Journal*, Vol. 9, No. 757, C1, 08-1134, Sept. 2009 (in Japanese).

[3] Budi Rachmanto, Kenzo Nonami, ”Zero Bias MIMO Simple Adaptive Control on Low-Loss Homopolar Flywheel with Active Magnetic Bearings”, *Dynamics and Design Conference 2008, CD-ROM Proc.*, 661, Japan Soc. of Mech. Eng., Sept. 2008 (in Japanese).

[4] Johnson, D., Brown, G.V., and Inman, D.J., ”Adaptive Variable Bias Magnetic Bearing Control”, *Proc. of American Control Conference*, Vol. 4, pp. 2217-2223, Philadelphia, USA, 1998.

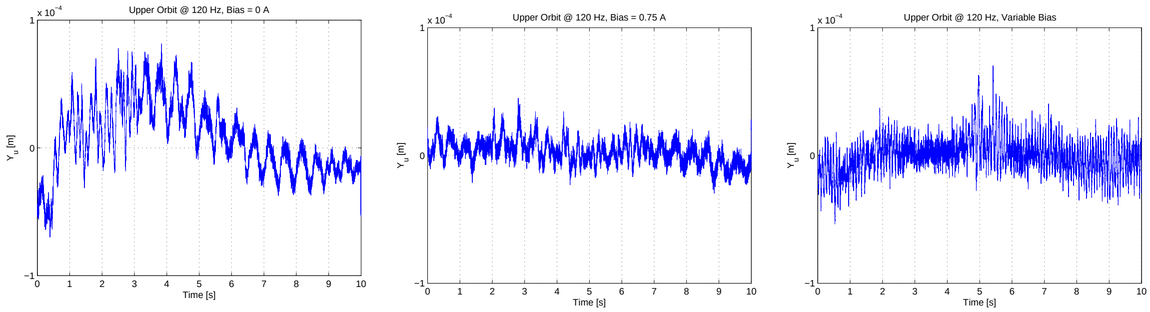

(a) zero bias (b) fixed bias: 0.75A (c) variable bias

Fig. 5 Flywheel orbits while EV is moving

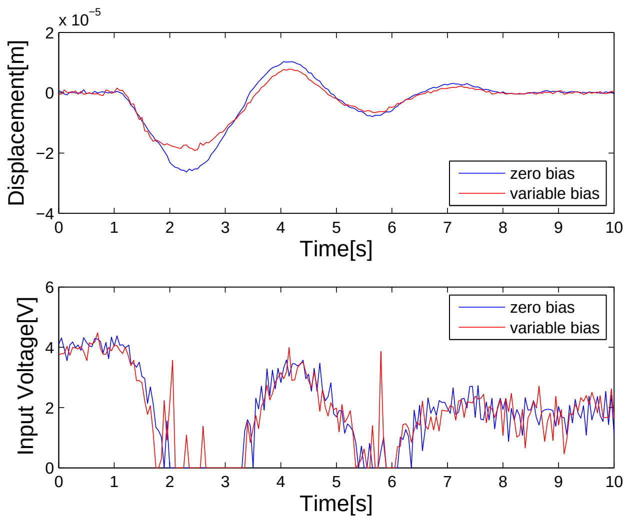

Fig. 6 Flywheel displacements comparison